

# Study of photocatalyst magnesium aluminate spinel nanoparticles

Atikur Rahman · R. Jayaganthan

Received: 23 August 2014 / Accepted: 27 October 2014 / Published online: 18 March 2015  
© The Author(s) 2015. This article is published with open access at Springerlink.com

**Abstract** Magnesium aluminate spinel nanoparticles with different concentration of alumina ( $x = 0.1, 0.2, 0.3, 0.4$  and  $0.54$ ) are synthesized by solid state reaction method. The synthesized products are characterized by powder X-ray diffraction and UV–Vis spectroscopy. The prepared nanoparticles exhibit a cubic structure with average crystallite size 25.4, 30.1, 31.2, 29.6 and 19.5 nm, respectively. The band gap values of magnesium aluminate spinel nanoparticles are found to increase with increase in alumina concentration ( $x = 0.1$  to  $0.54$ ). Photocatalytic studies of the magnesium aluminate spinel nanoparticles are done by taking methylene blue as pollutants. Their degradation behavior has been discussed.

**Keywords** XRD · Spectrophotometer · Photocatalyst

## Introduction

Textile industry uses large volumes of water in wet processing operations resulting in generation of substantial quantities of wastewater which contain large amount of dyestuff. Although these dyes are an important part of textile industry but their discharge in water bodies is very complicated as these are highly toxic and have

carcinogenic effects on human health [1, 2]. Till now, many methods (chemical, physical, biological) have been developed to overcome this problem. These methods have their own advantages and disadvantages. To overcome the disadvantages of these methods, development of a cost effective method is required which can effectively degrade the dyes without forming any sludge or other toxic substances. Semiconductor assisted photocatalytic degradation of dyes, which is an advanced oxidation process has emerged as an important destructive technology that offers complete mineralization of most of the organic pollutants and thus there is no further requirement for secondary disposal methods [3]. Some spinel-type oxides such as  $\text{BaCr}_2\text{O}_4$  [4],  $\text{NiFe}_2\text{O}_4$  [5],  $\text{CaBi}_2\text{O}_4$  [6],  $\text{ZnGa}_2\text{O}_4$  [7],  $\text{CuGa}_2\text{O}_4$  [8],  $\text{ZnFe}_2\text{O}_4$  [9] and  $\text{CuAl}_2\text{O}_4$  [10] used as semiconductor Photocatalyst materials. Magnesium aluminate has been synthesized by various methods such as gel precursors [11], spray pyrolysis [12], co-precipitation [13], and freeze-drying [14]. Very limited literature is available on photocatalyst magnesium aluminate spinel by solid state reaction method. Therefore, in the present research work, magnesium aluminate spinel nanoparticles with different concentration of alumina ( $x = 0.1, 0.2, 0.3, 0.4$  and  $0.54$ ) have been synthesized by solid state reaction. It involves mixing of element or alloy powders with additives and lubricants, and the mixture is annealed in a controlled atmosphere furnace (at  $900^\circ\text{C}$ ) so as to bond the particles metallurgically [15]. Novelty of the process is the flexibility in weight from few grams to several kilograms can be produced in economically. The aim of the present research work is to study the effects of alumina doping concentration of magnesium aluminate spinel on its structural and optical by using XRD and UV–Vis spectrophotometer respectively. The photocatalytic degradation of the methylene blue dye on the magnesium aluminate spinel

---

A. Rahman (✉)  
Department of Metallurgical and Materials Engineering,  
National Institute of Technology Srinagar, Hazratbal,  
Srinagar 190006, India  
e-mail: atikurrhmn@gmail.com

R. Jayaganthan  
Department of Metallurgical and Materials Engineering &  
Centre of Nanotechnology, Indian Institute of Technology  
Roorkee, Roorkee 247667, India

particles is studied under UV light of 200 W. The mechanisms governing the photocatalytic properties of nanoparticles are elucidated in the present work.

## Experimental procedure

Magnesium aluminate spinel nanoparticles are synthesized via solid state reaction of MgO and Al<sub>2</sub>O<sub>3</sub> powders. The powders (99.5 %) reagent grade such as MgO and Al<sub>2</sub>O<sub>3</sub> are used. The mean particle sizes of MgO and Al<sub>2</sub>O<sub>3</sub> powders are 35 and 22 nm, respectively. A series of samples are prepared with mole fraction ( $x$ ) of Al<sub>2</sub>O<sub>3</sub> varying from 0.1 to 0.54 with step of 0.1. Appropriate amount of MgO and Al<sub>2</sub>O<sub>3</sub> powders are accurately weighed and ground thoroughly and repeatedly using an agate mortar and pestle to give about 10 g of the homogeneous powder in each case. Grinding of the powders is done in polyvinyl alcohol for 4 h in each case of the sample. Diethanolamine (Analytical Grade) is used as a binder. The resultant powdered samples are then precalcinated at 800 °C for 04 h. The precalcinated materials are again ground and annealed at 900 °C for 04 h followed by furnace cooling. XRD (Bruker AXS) measurements with CuK $\alpha$  radiation are performed to characterize the samples and to identify the different phases. The scan rate is used with a step of 0.01° and the scan range varies from 10–80°. The UV–Vis Optical transmission spectra of the magnesium aluminate nanoparticles have been studied by spectrophotometer (Perkin Elmer, Lambda 35) in the wavelength ranges from 200 to 750 nm.

## Photocatalytic activities measurements

In the laboratory photocatalytic degradation is investigated in glass beaker (250 mL) under the UV light using a 200 W. The solution for photo degradation measurement is prepared by adding 0.1 g/L of magnesium aluminate nanoparticles + 10 mg/L of methylene blue dye + 100 mL of water. Prior to illumination, the suspension is magnetically stirred continuously in the dark for 1 h to disperse the catalyst and establish an adsorption/desorption equilibrium. After that, the suspension is irradiated with UV light. During irradiation process, stirring is continued to keep the mixture in suspension. At given time intervals of irradiation, 5 mL of the dye solution is sampled and centrifugated immediately to remove the magnesium aluminate nanoparticles. The change in methylene blue dye concentration in each photo degraded solution is monitored by two sets of measurements. Firstly, the maximum absorbance of methylene blue dye is measured at  $\lambda_{\text{max}} = 270$  nm in an ultraviolet–visible (UV–Vis) spectrometer (Perkin Elmer Lambda 35). Secondly, the total

organic carbon is determined by CHN analyzer (Elementar Vario EL III). Prior to the total organic carbon determination, the solution is filtered through a filter of 0.2  $\mu\text{m}$  pore size to remove photocatalysts.

## Results and discussion

### X-ray diffraction (XRD)-structural studies

X-ray diffraction patterns are analyzed to get an idea of the influence of different concentration of alumina on the crystal structure and the crystallite size of the magnesium aluminate nanoparticles. Figure 1 shows the XRD pattern of magnesium aluminate with different concentration of alumina ( $x = 0.1, 0.2, 0.3, 0.4$  and  $0.54$ ). XRD patterns of these samples exhibit peaks corresponding to (111), (012), (220), (312), (311), (222), (400), (113), (331), (422), (511), (018), (440), (214), (620), and (622) planes, which can be indexed as for cubic spinel structure according to PCPDFWIN CAS Number: PDF#860084. The (400) peak shows the highest intensity in all cases, implying that all the samples have a cubic spinel structure with a preferred orientation. There are no detectable diffraction peaks for Al metal clusters, Al or Mg oxide secondary phases or other impurity phases within the sensitivity of our XRD measurements, implying that single phase of MgAl<sub>2</sub>O<sub>4</sub> spinel has formed in MgO–Al<sub>2</sub>O<sub>3</sub> system. The mean crystallite size is determined from the broadening of the diffraction peaks (311) and (400) plane using Debye–Scherrer's formula [16]. Instrumental broadening has been accounted for the calculation of grain size, and its value of 0.1 (for standard Si sample) has been subtracted from the full-width half maximum (FWHM) value, from  $B$  value. Table 1 represents the  $2\theta$ , full width at half maximum (FWHM)

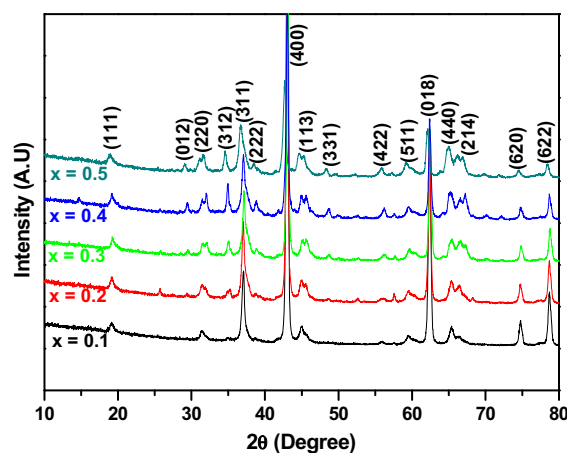


**Fig. 1** XRD pattern of magnesium aluminate spinel nanoparticles with different alumina doping concentration ( $x = 0.1, 0.2, 0.3, 0.4$  and  $0.54$ )

**Table 1** The  $2\theta$  and full width half maximum (FWHM) values, cell parameters ‘ $a$ ’,  $d$  Value and average crystal size ( $D$ ) of magnesium aluminate spinel nanoparticles with different alumina doping concentration ( $x = 0.1, 0.2, 0.3, 0.4$  and  $0.54$ )

Mole fraction of Alumina ( $x$ )	$2\theta$ Value (deg)	FWHM (deg)	Cell parameter ( $a$ ) (Å)	$d$ Value (Å)	Average crystal size $D$ (nm)
0.00	44.014	0.332	8.4012	2.1003	25.4
0.2	44.019	0.281	8.4048	2.1012	30.1
0.3	44.121	0.270	8.3864	2.0966	31.2
0.4	44.012	0.285	8.3992	2.0998	29.6
0.54	43.681	0.431	8.4668	2.1167	19.5

values, cell parameters ‘ $a$ ’,  $d$  value and average crystal size ( $D$ ). Therefore, the increase in lattice parameters (Table 1) and the decrease in average crystallite size could be understood by formation of  $\text{MgAl}_2\text{O}_4$  spinel phase.

Formation of magnesium aluminate spinel from its constituent oxides is a counter diffusion process of  $\text{Al}^{3+}$  and  $\text{Mg}^{2+}$  ions [17]. Magnesium aluminate spinel formation is based on the Wagner mechanism [18], oxygen ions remain at the initial sites. In order to keep electroneutrality, 3  $\text{Mg}^{2+}$  diffuse towards the alumina side and 2  $\text{Al}^{3+}$  diffuses towards the magnesia side, so four  $\text{MgO}$  change to one magnesium aluminate spinel at the  $\text{MgO}$  side and four  $\text{Al}_2\text{O}_3$  change to three magnesium aluminate spinel. Reduction of particle size can decrease the distance between vacancy sites (or that of grain boundaries) and enhance the vacancy diffusion to external surface and thus help formation of magnesium aluminate spinel and grain growth.

### Optical studies

The optical transmission spectra are recorded using UV visible spectrophotometer (Perkin Elmer, Lambda 35). These measurements are performed using air as reference in a wavelength range of 200–750 nm. As sources for visible and UV radiations, Halogen and deuterium lamp are used. The effects of different alumina concentration ( $x = 0.1, 0.2, 0.3, 0.4$  and  $0.54$ ) on the optical absorbance spectra in the visible range of magnesium aluminate spinel nanoparticles are presented in Fig. 2a. The optical band gap energy values  $E_g$  of the magnesium aluminate spinel nanoparticles with different concentration of alumina ( $x = 0.1, 0.2, 0.3, 0.4$  and  $0.54$ ) is determined by Tauc relationship [19]. The estimated energy gap for the magnesium aluminate nanoparticles with alumina concentration  $x = 0.1$  is 5.25 eV, it is increased to 5.29 eV for alumina concentration  $x = 0.2$  and it further increases to 5.37 eV for alumina concentration  $x = 0.54$ . The energy

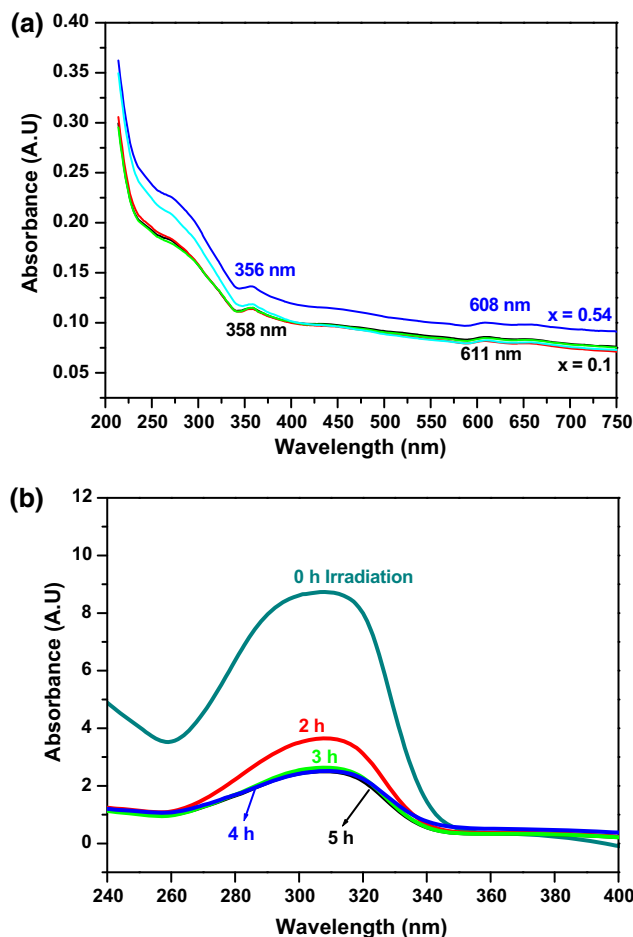


**Fig. 2** a Optical absorbance spectra of magnesium aluminate spinel nanoparticles with different alumina doping concentration ( $x = 0.1, 0.2, 0.3, 0.4$  and  $0.54$ ), and b UV–Vis spectral changes of Methylene blue dye solution during the photocatalytic degradation by magnesium aluminate spinel nanoparticles with alumina concentration  $x = 0.54$  under UV light

band gap of magnesium aluminate spinel nanoparticles observed in the present work is in accordance with the results of Suresh et al. [20]. The increase in band gap is due to doping effects and formation of  $\text{MgAl}_2\text{O}_4$  spinel phase. The change in optical band gap can be explained in terms of Burstein–Moss band gap widening and band gap narrowing due to the electron–electron and electron–impurity scattering [21].

Some spinel-type oxides are used as photocatalyst. The requirement of photocatalyst is as follows:

- (i) The optical absorbance of the spinel oxide should be more as much as possible in the visible range from 400 to 800 nm, in order to minimize the optical loss and obtain higher efficiency.
- (ii) The energy band gap should be more than 3.00 eV, so that it reduces the recombination losses at the photocatalyst surface.



Magnesium aluminate spinel with alumina concentration  $x = 0.54$  exhibits better quantum confinement due to its smaller particle size, 19.5 nm as compared to magnesium aluminate spinel with alumina concentration ( $x = 0.1, 0.2, 0.3$  and  $0.4$ ) as observed in the present work. It is evident that the band gap is influenced by size effect of nanoparticles and alters the density of states, which in turn affects the optical properties.

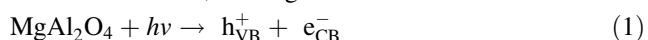
#### Photocatalytic activities of magnesium aluminate spinel nanoparticles

Photocatalytic study of magnesium aluminate spinel nanoparticles with alumina ( $x = 0.54$ ) concentration is done using methylene blue dye under UV light irradiation. In the present work magnesium aluminate spinel nanoparticles with alumina ( $x = 0.54$ ) concentration has been chosen, because it has the lowest crystallite size (19.5 nm) as compared to alumina concentration ( $x = 0.1, 0.2, 0.3$  and  $0.4$ ). Figure 2b shows degradation of methylene blue dye under UV-irradiation at different reaction times (from 0 to 5 h). Degradation of dye is indicated by decrease in absorbance intensity of samples with the increase of exposed time. Around 88.0 % of the methylene blue dye decomposed under UV light within 5 h. The photocatalytic degradation of methylene blue under magnesium aluminate spinel nanoparticles with alumina ( $x = 0.54$ ) in terms of change in concentration with respect to the initial concentration is shown in Fig. 3a. The value of rate constant ( $K$ ) for photochemical reactions is obtained from the slope of plot of Fig. 3b. The degradation kinetics can be simplified to pseudo first order kinetic equation  $\ln(C_a/C_t) = K \times t$ .

where  $C_t$  is the concentration of dye after irradiation in selected time interval,  $C_a$  the initial concentration of dye,  $K$  the first-order rate constant and  $t$  the irradiation time. By linear fitting of slope of plot of Fig. 3b, the value of  $K$  estimated to be  $0.2157 \text{ min}^{-1}$ .

Photocatalytic degradation mechanism of methylene blue dye on of magnesium aluminate nanoparticles:

When the magnesium aluminate spinel ( $\text{MgAl}_2\text{O}_4$ ) photocatalyst absorbs a photon, an electron transfers from the VB to the CB, leaving a hole in VB:



The hole can be trapped by chemisorbed water or surface hydroxyl groups to form  $^*\text{OH}$  radical. On the other hand, electrons can be trapped by the molecular oxygen absorbed on the surface of catalyst to produce superoxide anion radicals ( $\text{O}_2^{\bullet -}$ ), which then react with water to form  $^*\text{OH}$  radical.  $^*\text{OH}$  radical or  $\text{O}_2^{\bullet -}$  reacts with methylene blue dye leads to the mineralization of the pollutants. Holes and electrons all can cause to the degradation of methylene

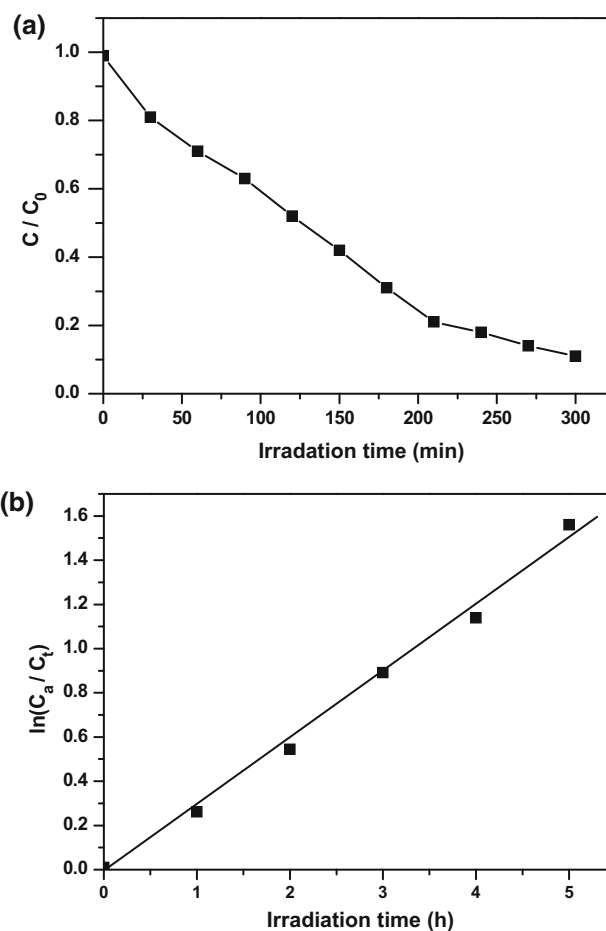


**Fig. 3** a Photo catalytic degradation of methylene blue dye solution by magnesium aluminate spinel nanoparticles with alumina concentration  $x = 0.54$  under UV light irradiation **b** reaction kinetics of photocatalytic degradation by magnesium aluminate spinel nanoparticles with alumina concentration  $x = 0.54$  under UV light irradiation

blue. Thus  $^*\text{OH}$  and  $\text{O}_2^{\bullet -}$  radical both are responsible and worked together to degrade the methylene blue dye.

The photocatalytic activity of magnesium aluminate spinel nanoparticles is strongly dependent on the dopants concentration. Increasing the doping concentrations of alumina increases the energy band gap, and reduces the crystallite size due to formation of single phase of  $\text{MgAl}_2\text{O}_4$  spinel, which results the enhanced optical absorption spectra. The presence of  $\text{MgAl}_2\text{O}_4$  spinel phase in  $\text{MgO-Al}_2\text{O}_3$  system can also play an important role in efficient charge separation [22]. In  $\text{MgO-Al}_2\text{O}_3$  system, the presence of  $\text{MgAl}_2\text{O}_4$  phase hetero junction may decrease the recombination of e–h pairs. This increases the availability of the electrons (holes) to migrate to the magnesium aluminate surface of the photocatalysts and consequently improves the occurrence of redox process (electrons reduce dissolved molecular oxygen to super oxide radical anions while holes forms hydroxyl radicals). In the present work, Magnesium aluminate spinel nanoparticles with alumina concentration  $x = 0.54$  has

highest optical absorbance due to lowest particles size (19.5 nm). Magnesium aluminate spinel is an ideal candidate for replacing TiO<sub>2</sub>, TiO<sub>2</sub> doped ZnO, Ag doped ZnO, SnO<sub>2</sub> (Tin oxide), and Indium tin oxide (ITO), because:

- (i) Indium is very scarce and expensive material.
- (ii) TiO<sub>2</sub> and Ag are also expensive.
- (iii) Indium tin oxide (ITO) is not stable within silane plasma,

SnO<sub>2</sub> (Tin Oxide) has also similar limitations as that of Indium tin oxide (ITO).

On the other hand, magnesium aluminate spinel is non-toxic, low cost material and has high thermal stability. It exhibit higher absorbance, higher optical energy band gap and similar photo degradation as observed in TiO<sub>2</sub>, TiO<sub>2</sub> doped ZnO, Ag doped ZnO, SnO<sub>2</sub> (Tin oxide) and Indium tin oxide (ITO).

## Conclusions

Magnesium aluminate spinel nanoparticles with different alumina concentration ( $x = 0.1, 0.2, 0.3, 0.4$  and  $0.54$ ) have been successfully synthesized by solid state reaction method. The effect of alumina concentration on crystallite size, optical and photo catalytic properties are studied. The increase of lattice constants and the reduction in average crystalline size could be understood by formation of single phase MgAl<sub>2</sub>O<sub>4</sub> spinel. Optical absorption and energy band gap of magnesium aluminate spinel nanoparticles increases with increasing the alumina doping concentration, which results into increased the photocatalytic activity, due to decrease the recombination of e–h pairs. The magnesium aluminate spinel nanoparticles showed photocatalytic activity by degradation of 88.0 % of the methylene blue dye under UV light radiation within 5 h. It may be highlighted that magnesium aluminate spinel nanoparticles can be obtained by using a low cost solid state reaction method (in few grams to Kgs) and can be used as photocatalyst in place of Ag<sub>2</sub>O doped ZnO, Cu doped ZnO, Ag doped TiO<sub>2</sub>, W doped TiO<sub>2</sub>, TiO<sub>2</sub>, TiO<sub>2</sub> doped ZnO, SnO<sub>2</sub> (Tin oxide), and Indium tin oxide (ITO) due to their good optical properties, high thermal and chemical stability.

**Open Access** This article is distributed under the terms of the Creative Commons Attribution License which permits any use, distribution, and reproduction in any medium, provided the original author(s) and the source are credited.

## References

1. Ismail, B., Hussain, S.T., Akram, S.: Adsorption of methylene blue onto spinel magnesium aluminate nanoparticles: adsorption isotherms, kinetic and thermodynamic studies. *Chem. Eng. J.* **219**, 395–402 (2013)

2. Piccin, S.J., Gomes, C.S., Feris, L.A., Gutterres, M.: Kinetics and isotherms of leather dye adsorption by tannery solid waste. *Chem. Eng. J.* **183**, 30–38 (2012)
3. Firooz, A.A., Mahjoub, A.R., Khodadadi, A.A., Movahedi, M.: High photocatalytic activity of Zn<sub>2</sub>SnO<sub>4</sub> among various nanostructures of Zn<sub>2</sub>xSn<sub>1-x</sub>O<sub>2</sub> prepared by a hydrothermal method. *Chem. Eng. J.* **165**, 735–739 (2010)
4. Wang, D.F., Zou, Z.G., Ye, J.H.: A new spinel-type photocatalyst BaCr<sub>2</sub>O<sub>4</sub> for H<sub>2</sub> evolution under UV and visible light irradiation. *Chem. Phys. Lett.* **373**, 191–196 (2003)
5. Zhu, Z.R., Li, X.Y., Zhao, Q.D., Li, H., Shen, Y.: Porous “brick-like” NiFe<sub>2</sub>O<sub>4</sub> nanocrystals loaded with Ag species towards effective degradation of toluene. *Chem. Eng. J.* **165**, 64–70 (2010)
6. Tang, J.W., Zou, Z.G., Ye, J.H.: Angew. efficient photocatalytic decomposition of organic contaminants over CaBi<sub>2</sub>O<sub>4</sub> under visible-light irradiation. *Chem. Int. Ed.* **43**, 4463–4466 (2004)
7. Boppana, V.B.R., Doren, D.J., Lobo, R.F.: A spinel oxynitride with visible-light photocatalytic activity. *ChemSuschem* **3**, 814–817 (2010)
8. Gurunathan, K., Baeg, J.O., Lee, S.M., Subramanian, E., Moon, S.J., Kong, K.J.: Visible light active pristine and Fe<sup>3+</sup> doped CuGa<sub>2</sub>O<sub>4</sub> spinel photocatalysts for solar hydrogen production. *Int. J. Hydrog. Energy* **33**: 2646–2652 (2006)
9. Cao, S.W., Zhu, Y.J., Cheng, G.F., Huang, Y.H.: ZnFe<sub>2</sub>O<sub>4</sub> nanoparticles: microwave-hydrothermal ionic liquid synthesis and photocatalytic property over phenol. *J. Hazard. Mater.* **171**, 431–435 (2009)
10. Liu, W.Z., Liu, B., Qiu, Q., Wang, F., Luo, Z.K., Zhang, P.X., Wei, S.H.: Synthesis, characterization and photocatalytic properties of spinel CuAl<sub>2</sub>O<sub>4</sub> nanoparticles by a sonochemical method. *J. Alloys Compd.* **479**, 480–483 (2009)
11. Walker, Jr, Owens, E.H., Etienne, J.W., Walker, M.D.: The novel low temperature synthesis of nanocrystalline MgAl<sub>2</sub>O<sub>4</sub> spinel using gel precursors. *Mater. Res. Bull.* **37**, 1041–1050 (2002)
12. Suyama, Y., Kato, A.: Characterization and sintering of magnesium aluminate spinel prepared by spray-pyrolysis technique. *Ceram. Int.* **8**, 17–21 (1982)
13. Bratton, R.J.: Coprecipitates yielding MgAl<sub>2</sub>O<sub>4</sub> spinel powders. *Am. Ceram. Soc. Bull.* **48**, 759–762 (1969)
14. Wang, C.T., Lin, L.S., Yang, S.J.: Preparation of MgAl<sub>2</sub>O<sub>4</sub> spinel powders via freeze-drying of alkoxide precursors. *J. Am. Ceram. Soc.* **75**(8), 2240–2243 (1992)
15. Fan, Y., Lu, X.B., Ni, Y.W., Zhang, H.J., Zhu, M.W., Li, Y.J.P.: Catalytic destruction of chlorinated aromatic pollutants over mesoporous Cu<sub>x</sub>Mg<sub>1-x</sub>Al<sub>2</sub>O<sub>4</sub> spinel oxides. *Chem. Appl. Catal. B: Environ.* **101**, 606–612 (2011)
16. Zou, D., Yan, D., Xiao, L., Dong, Y.: Characterization of nanostructured TiN coatings fabricated by pulse laser. *Surf. Coat. Technol.* **202**, 1928–1934 (2008)
17. Carter, R.E.: Mechanism of solid state reaction between MgO-Al<sub>2</sub>O<sub>3</sub> and MgO-Fe<sub>2</sub>O<sub>3</sub>. *J. Am. Ceram. Soc.* **44**(3), 116–120 (1961)
18. Wagner, C., Koch, E.: Formation of Ag<sub>2</sub>HgI<sub>4</sub> from AgI and HgI<sub>2</sub> by reaction in solid state. *Ibid. B.* **34**, 317–321 (1936)
19. Wang, R.C., Lin, H.Y.: Cu doped ZnO nanoparticle sheets. *Mater. Chem. Phys.* **125**, 263–266 (2011)
20. Sampath, S.K., Kanhere†, D.G., Pandey, R.: Electronic structure of spinel oxides: zinc aluminate and zinc gallate. *J. Phys.: Condens Matter.* **11**:3635–3644 (1999)
21. Sernelius, B.E., Berggren, K.F., Jin, Z.C., Hamberg, I., Granavist, C.G.: Band-gap tailoring of ZnO by means of heavy Al doping. *Phys. Rev. B* **37**, 10244–10248 (1988)
22. Zou, C.W., Yan, X.D., Han, J., Chen, R.Q., Bian, J.M., Haemmerle, E., Gao, W.: Preparation and enhanced photoluminescence property of ordered ZnO/TiO<sub>2</sub> bottlebrush nanostructures. *Chem. Phys. Lett.* **476**, 84–88 (2009)

